TÜBİTAK

Turkish Journal of Earth Sciences

http://journals.tubitak.gov.tr/earth/

Research Article

Turkish J Earth Sci
(2017) 26: 302-313
© TÜBİTAK
doi:10.3906/yer-1702-3

Karstic depressions on Bolkar Mountain plateau, Central Taurus (Turkey): distribution characteristics and tectonic effect on orientation

Muhammed Zeynel ÖZTÜRK[1,*], Mesut ŞİMŞEK[2], Mustafa UTLU[3], Mehmet Furkan ŞENER[1]

[1]Department of Geography, Faculty of Arts and Sciences, Niğde Ömer Halisdemir University, Niğde, Turkey
[2]Department of Physical Geography, Graduate School of Social Sciences, İstanbul University, İstanbul, Turkey
[3]Department of Geography, Faculty of Arts and Sciences, İstanbul University, İstanbul, Turkey

Received: 07.02.2017 • **Accepted/Published Online:** 21.08.2017 • **Final Version:** 29.09.2017

Abstract: This study investigates the spatial distribution characteristics of karstic depressions that developed on a 2558 km^2 plateau with gently sloping in neritic (reef) limestones in the western section of the Bolkar Mountains. The 30,132 karstic depressions identified are located at elevations between 1315 and 2525 m, while 31°/km^2 slope and 5.6 km/km^2 drainage density are limited to the spatial distribution of depressions. In the central section of the study area at the anticlinal surface, maximum density (99 depressions/km^2) is reached between elevations of 1930 and 2080 m. The orientation of depressions is predominantly NE–SW. However, in the same area, the orientation of depressions also varies from ENE–WSW toward NE–SW from west to east. The left-lateral strike–slip Ecemiş Fault was effective in the formation of these orientations, with a NE–SW orientation close to the fault and ENE–WSW orientation farther away from the fault.

Key words: Karstic depressions, density, orientation, tectonics, Ecemiş fault

1. Introduction

Karstic terrains have distinctive hydrology and surface and subsurface landforms. Large areas of the ice-free continental area of the Earth, especially in the northern hemisphere, are underlain by karst developed in carbonates rocks (Ford and Williams, 2007). Karst morphology is a significant component of the physical geography of the Mediterranean region (Lewin and Woodward, 2009) and Turkey. Karstic terrains covering about one third of Turkey spread almost over the entire country (Günay, 2010; Nazik and Tuncer, 2010). The largest and most important karstic terrain is the Taurus Mountains, forming a continuous karst belt across southern Turkey. The Taurus Mountain range is highly karstified due to abundance of carbonate rocks, and tectonic activity and climatic conditions present and past, especially glacial and interglacial times in the Quaternary (Klimchouk et al., 2006). Most of the karstic landforms follow structural lineaments on the Taurus Mountains (Elhatip, 1997; Gunn and Günay, 2004).

Circular or semicircular karstic depressions varying in diameter from a few meters to 1 km (Ford and Williams, 2007) are characteristic landforms in the Taurus karst region of Turkey (Elhatip, 1997; Öztürk et al., 2015). Limestones with more than 90% $CaCO_3$ (Nazik, 1986) and a thickness of up to 5000 m in the Taurus Mountain belt (Koçyiğit, 1984) resulted in appropriate lithologic conditions for depressions formed by the dissolution of limestone. Within the same lithologic unit, gently sloping karstic plateaus over 2000 m provide appropriate topographic conditions because depressions generally reach maximum density on the gentle slopes of high karstic plateaus (Plan and Decker, 2006; Faivre and Pahernik, 2007; Sauro, 2013; Daura et al., 2014; Bocic et al., 2015). Tectonic structure, especially fracture intensity and orientation, has a strong effect on doline development, density, and distribution on gently sloping high karstic plateaus (Car, 2001; Jemcov et al., 2001; Doctor and Doctor, 2012). Although some studies emphasize that there are a great many depressions found in the study area, the actual number, spatial distribution, morphometric properties, and the relationship with tectonic evolution of the depressions are unknown. The aims of this study are (1) to determine the spatial distribution and morphometric properties of the depressions and, (2) to explain the effect of tectonic evolution on the formation of these features in the western section of the Bolkar Mountains in the Central Taurus Mountains (Figure 1). The morphometric characteristics of the depressions in the Central Taurus are

* Correspondence: muhammed.zeynel@gmail.com

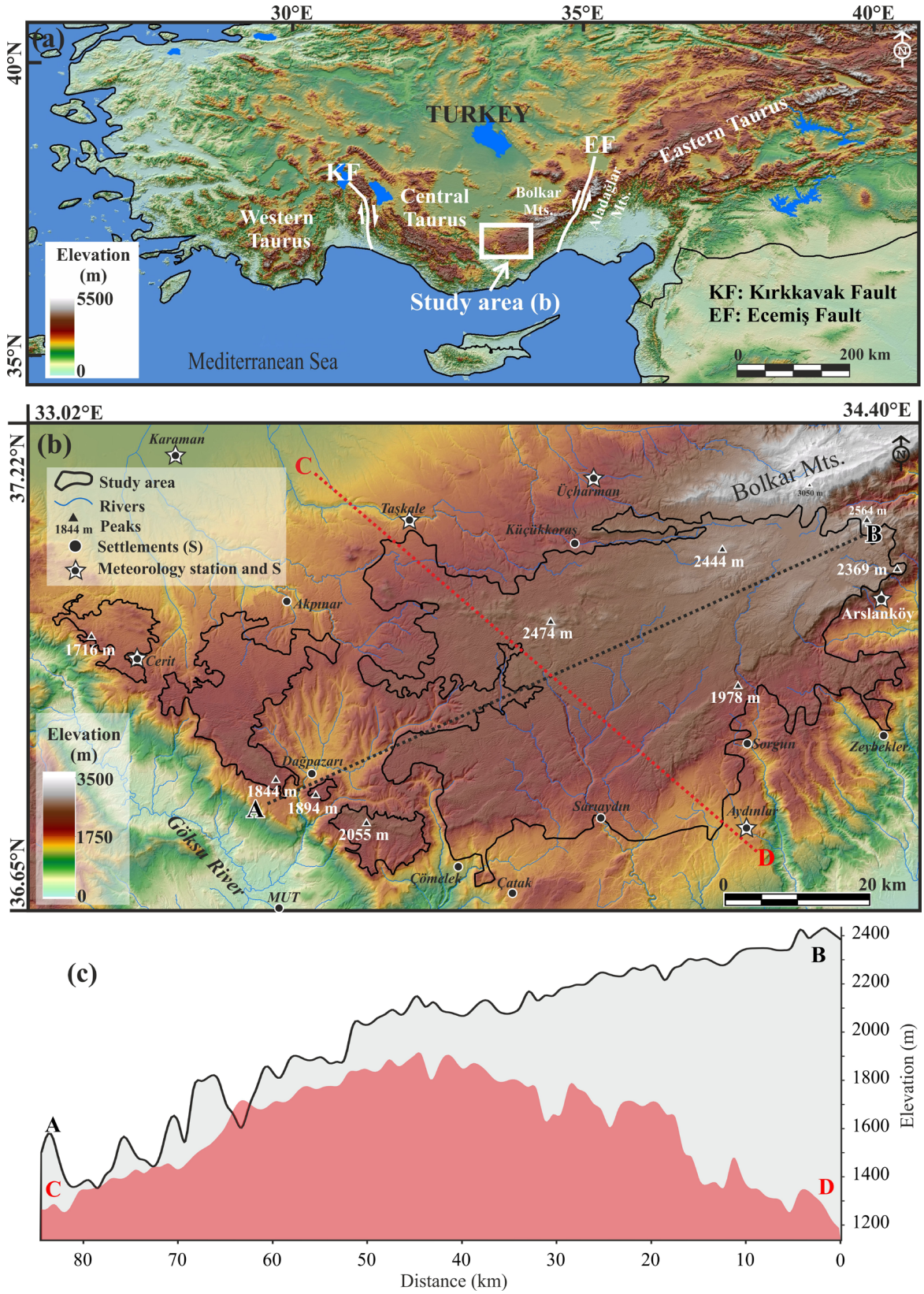


Figure 1. (a) Geographical classification of Taurus Mountains (Özgül, 1984), (b) location of study area, (c) digital elevation model of study area.

discussed in detail and the roles of tectonics, slope, and drainage conditions in the study area are analyzed for the first time.

2. Study area

At the south of the Anatolian Plateau, the Taurus Mountains extend in an east–west direction for about 1300 km and are divided into three basic regions by the Kırkkavak fault to the west and the Ecemiş fault to the east (Özgül, 1984; Dhont et al., 1999) (Figure 1a). The study area is located in the Central Taurus Mountains and contains the Aksıfat, İbrala, Sertavul, and Dümbelek Düzlüğü plateaus, which are located between the River Göksu and the Bolkar Mountains, comprises a 2558 km^2, gently sloping NE–SW-oriented anticlinal surface (Figure 1b). The elevation of the study area increases from 1200 m in the west to 2550 m in the east (Figure 1c). About 70% of the area is located between 1550 and 2100 m elevations. According to data from the Karaman (1025 m), Üçharman (1329 m), Aydınlar (1346 m), Taşkale (1473 m), Cerit (1538 m), and Arslanköy (1650 m) meteorological stations, the annual mean temperature varies between 11.9 and 9.4 °C, while total precipitation varies between 322 and 788 mm.

The base units of study area are composed of Cretaceous limestones and ophiolitics. The Upper Oligocene Göcekler formation, which is composed of red mudstone, claystone, and sand stones defined by Özdoğan (1999) and the Fakirca formation, which consists of clayey limestone and shale with siltstone bands as defined by Gedik et al. (1979), unconformably overlie these Cretaceous units. The Derinçay formation, which is composed of sandstone, conglomerate, red mudstone, gray sand, and mudstone intercalation derived from ophiolite and older limestones as described by Gedik et al. (1979), unconformably overlies Upper Oligocene units. Over all of these units, the Middle Miocene Mut formation and the Middle-Upper Miocene Tirtar formation, which are composed of neritic limestone and clayey limestone alternations described by Gedik et al. (1979) and Atabey et al. (2000), unconformably overlie. The investigated unit of the Mut Formation, which constitutes the top of the section, has a thickness of 940 m. Moderate and thick layers comprise fossiliferous limestones with intercalations of clayey, silty, and sandy units (Özkale et al., 2007) (Figure 2). The depressions investigated within the study area (Figure 3) that developed on this Middle-Upper Miocene limestone and clayey limestone units covering ~69% of the area have 5–10° dip values with broad and flattened folds (Şaroğlu et al., 1983).

3. Materials and methods

In this study, 1/25,000 scale topographic maps with 10-m contour interval are used to determine the spatial distribution and morphometric properties of the karstic depressions. For this purpose, the traditional method is used and the uppermost closed contour lines of depressions are delineated (Day, 1983; Denizman, 2003; Faivre and Pahernik, 2007; Telbisz et al., 2009; Benac et al., 2013; Bocic et al., 2015). The uppermost closed contour lines of 30,132 karstic depressions are digitized as polygons in a GIS framework and the morphometric properties of the polygons are calculated. With the aid of the polygons, the long and short axes of the shapes are drawn and elongation ratios (planimetric shape) are calculated and mapped. Additionally, to calculate the azimuth of the long axis, the orientation angles of the depressions are determined. Thus, for each shape, a data set comprising elevation, area, long and short-axis lengths, elongation ratio, circularity index, and orientation angle was created. The circularity index is a measure of the circularity of a depression. It is the ratio between the depression area and the area of a circle with the same perimeter (Denizman, 2003). Depth of depression is normally an important parameter but this parameter was not calculated in the current study because many of the depressions are shown with a single elevation contour. All active valley thalwegs are drawn on the topographic maps as polylines for drainage density. As these active valleys are not exposed to karstification, depression growth is not observed in these valley (Bocic et al., 2015).

The data set is examined in 1 km^2 (1 × 1 km) grids to determine depression and drainage density and slope values, and 25 km^2 (5 × 5 km) grids are used to create rose diagrams, in other words to determine the spatial distribution of orientation characteristics. Correlations between the depression density and slope angle, and drainage density are calculated. The programs Mapinfo, Geo Rose, and Corel DRAW are used for the mapping processes. Moreover, DJI Phantom 3 Pro is used for oblique air photos. The results of all analyses and field studies were evaluated together with the spatial distribution of karstic depressions and the tectonic and morphologic processes affecting the development of depressions.

4. Morphometric properties of depressions

The 30,132 depressions mapped on 1/25,000 scale maps in a 2558 km^2 area are located between the elevations of 1315 and 2525 m. The mean elevation of the depressions is 1944 m. However, the depression elevations are not homogeneously distributed within the elevation range considered. The number of depressions regularly increases up to 1850 m and then gradually decreases. More clearly, 75% of depressions are located between 1650 and 2250 m and the highest density of depressions by elevation (13.7%) is reached between 1800 and 1850 m. Density increases regularly up to 2100 m and reaches 19.3 depressions/km^2. The density is >10 depressions/km^2 between 1850 and 2450 m (Figure 4). In addition, a positive correlation

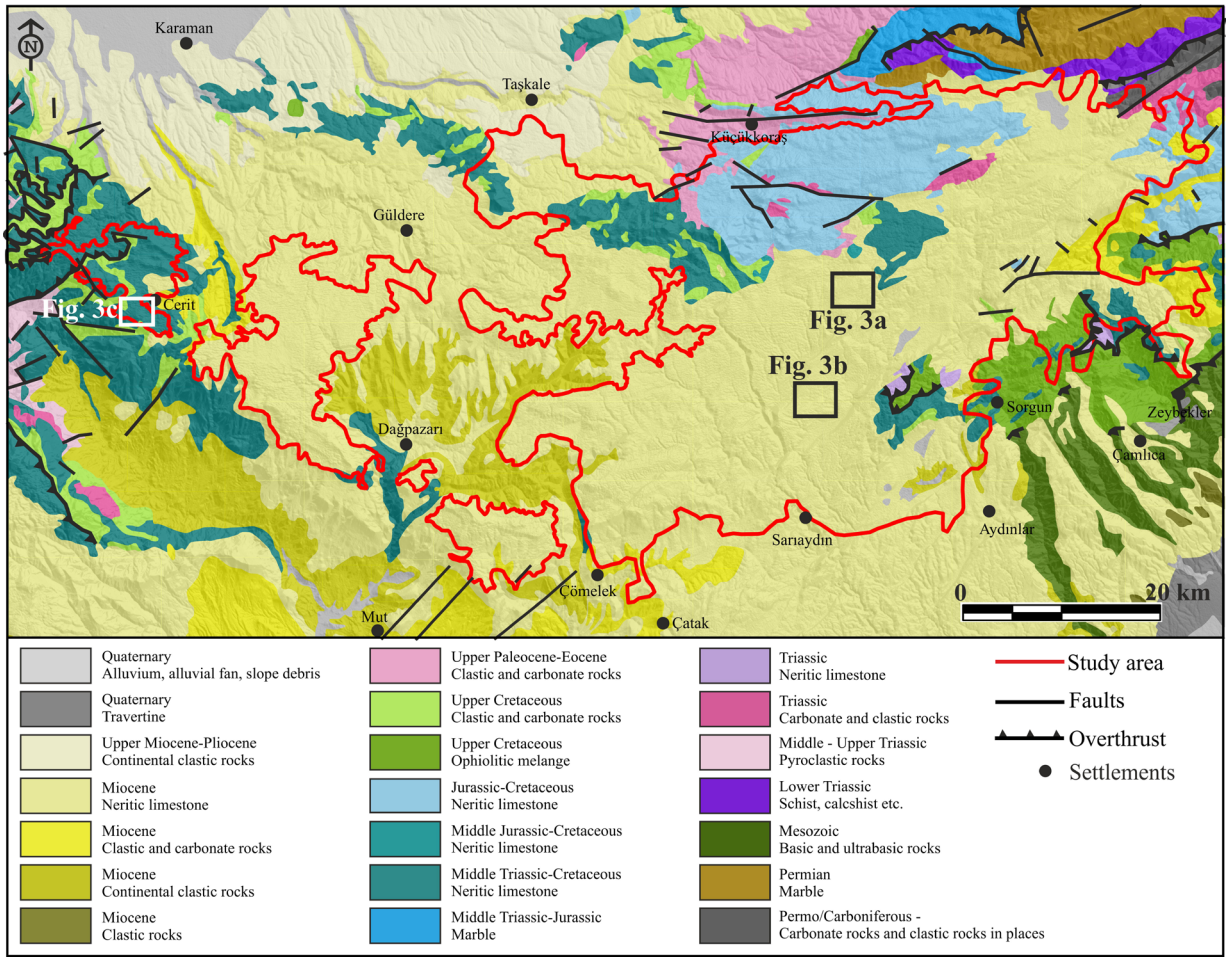


Figure 2. Geological map of study area (arranged from Şenel, 2002).

is observed between the depression density with the area of the contour interval that includes these depressions (r: 0.83).

With a mean density of 12 depressions/km^2 in the central section, coinciding with the anticlinal surface, the maximum density (99 depressions/km^2) was reached at elevations of 1930 to 2080 m (Figure 5a). In the area with maximum density, the mean long axis was 62 m with a mean short axis of 38 m and mean elongation ratio of 1.6 (Figure 5b). The mean elongation ratio is 1.9 and 89% of depressions have an elongation ratio between 1 and 3. However, the elongation ratio increases to 10 in the western section of the study area (Figure 5c). In the western portion of the area from 1595 to 1640-m high, the elongation ratio increases to 14 (Figure 5d). In this area, with broader coverage by depressions, the density is <10depressions/km^2.

The mean length of the long axis is 100 m and 89% of depressions have long-axis length less than 200 m. The mean length of the short axis is 49 m and 92% of depressions have short-axis length less than 100 m. The circularity index mean is 1.44 and 96% of depressions have a value between 1 and 3.

Drainage density and slope conditions are limiting factors affecting the distribution and density of depressions. There are negative correlations between depression density and drainage density, and depression density and slope angles, according to the gridded data (Figure 6). Maximum drainage density reaches 5.6 km/km^2 in the present study area according to the gridded data (Figures 6a and 6b). The mean slope angle (°/km^2) reaches 31° in a doline area according to the gridded data (Figures 6c and 6d). In other words, 31°/km^2 limits depression distribution. The same results are seen in the Dinaric karst of Slovenia (Gams, 2000). In general, areas with >10 depressions/km^2 density have drainage density and mean slope values less than 1 km/km^2 and 8°, respectively. The above results indicate clearly that the karstic depressions in the study area are developed mainly in gently sloping areas without active streams.

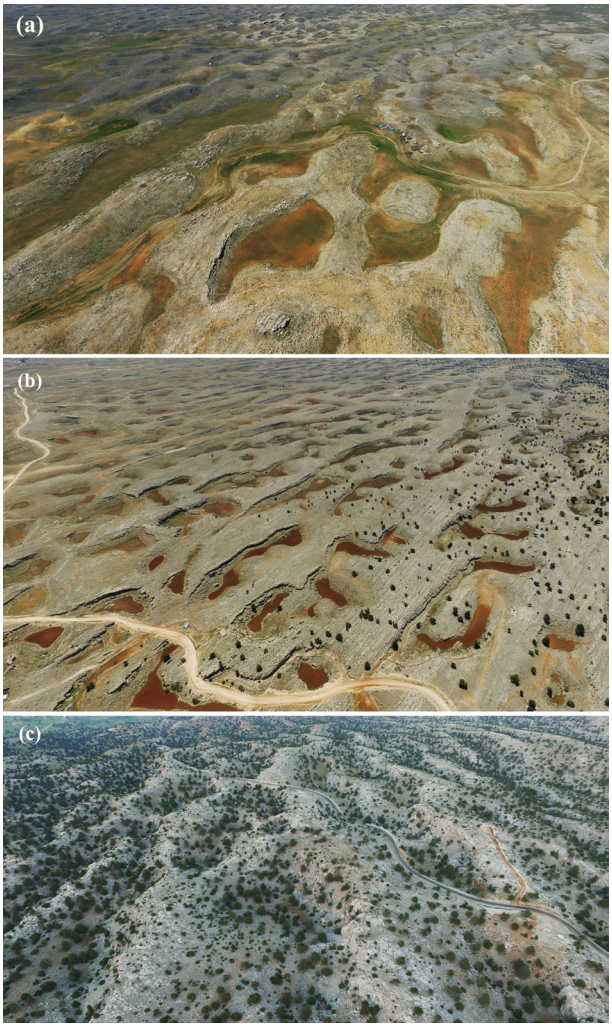


Figure 3. General views of Miocene limestones from the study area (locations shown in Figure 2).

Neritic limestones are the dominant lithological unit (90%) and the majority of the depressions (95.6%) occurred in this unit (Table). The majority of this lithological unit is Miocene (68.6%). Miocene neritic limestone comprises 69.1% of all depressions. However, the densest unit is Jurassic–Cretaceous neritic limestones (16.5 depressions/km^2) (Table). This situation is probably explained by weathering and tectonic activity for a long time on Jurassic–Cretaceous neritic limestones. More study is necessary about lithological effects on depression density.

5. Orientation of depressions and tectonic and geomorphologic evolution

The general orientation of the karstic depressions provides important evidence about the effective fracture and fault system (Faivre and Reiffsteck, 1999; Theilen-Willige et al., 2014); they are of great importance in the search for causes of tectonic and geomorphologic development in any karstic region (Mihljevic, 1994; Ekmekçi and Nazik, 2004; Closson and Karaki, 2009). In this context, the rose diagrams representing the distribution of the depression orientations in equally spaced parts of a study area provide evidence regarding the regional orientation of lineaments. In the present study, spatial distribution of the rose diagrams of depressions indicated a dominant NE–SW orientation (Figures 7a and 7b). This regional orientation is in agreement with the orographic elongation of the study area (Ardos, 1992), which is in line with the axis of the Taurus Mountains Belt. According to our field observations, the development of this NE–SW orientation seems to be controlled by commonly developed extensional fracture systems (Figures 7c–7e). However, the general trend of long-axis orientation shown in Figure

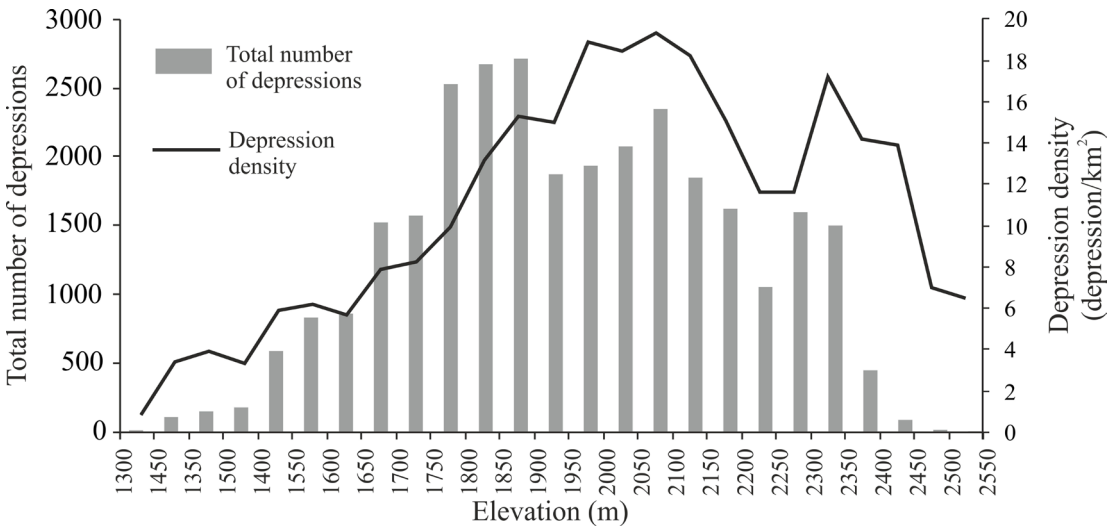


Figure 4. Density and total number of depressions.

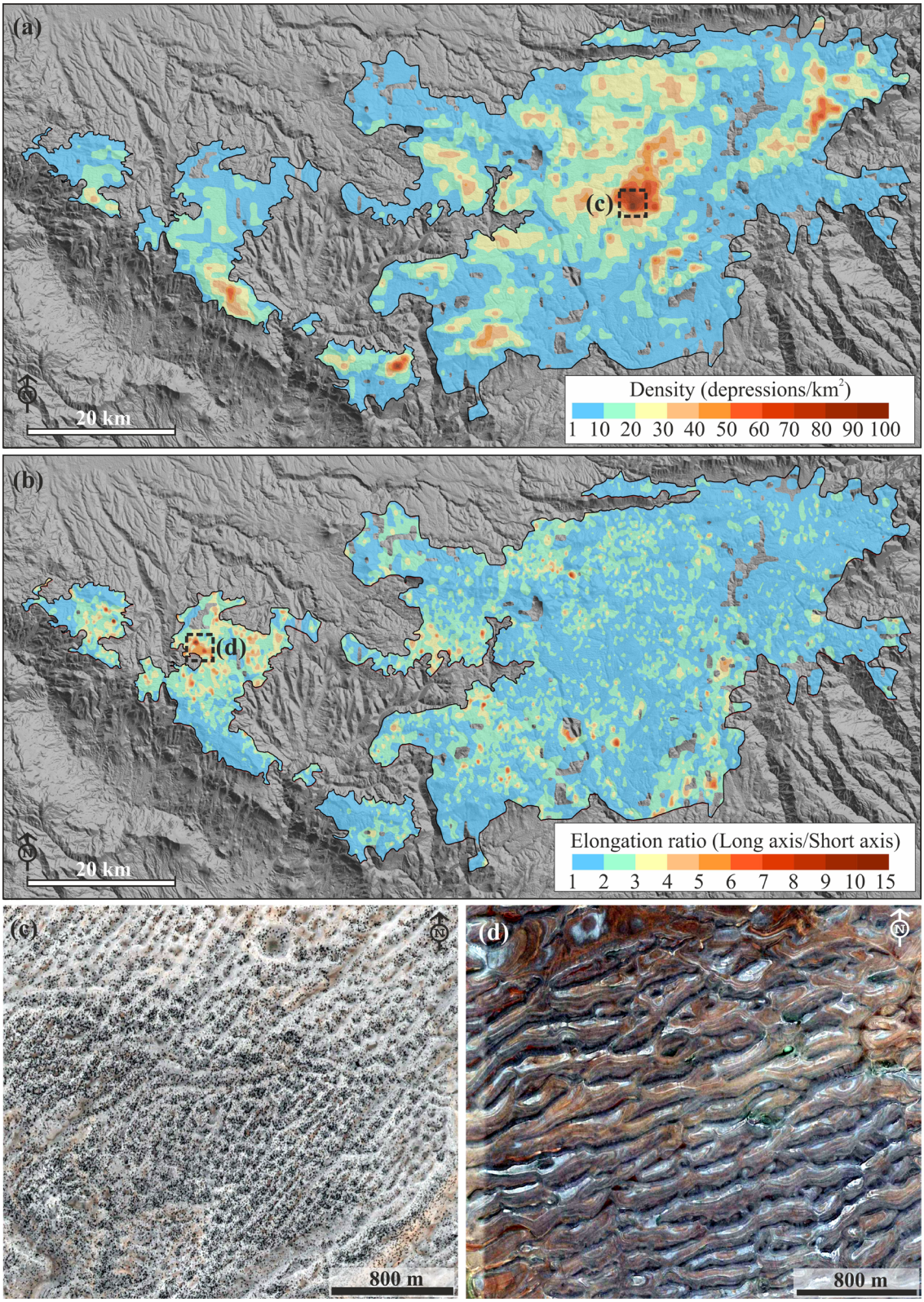


Figure 5. Distribution of (a) density and (b) elongation ratio. Satellite images of areas with maximum density (c) and elongation ratio (d), respectively.

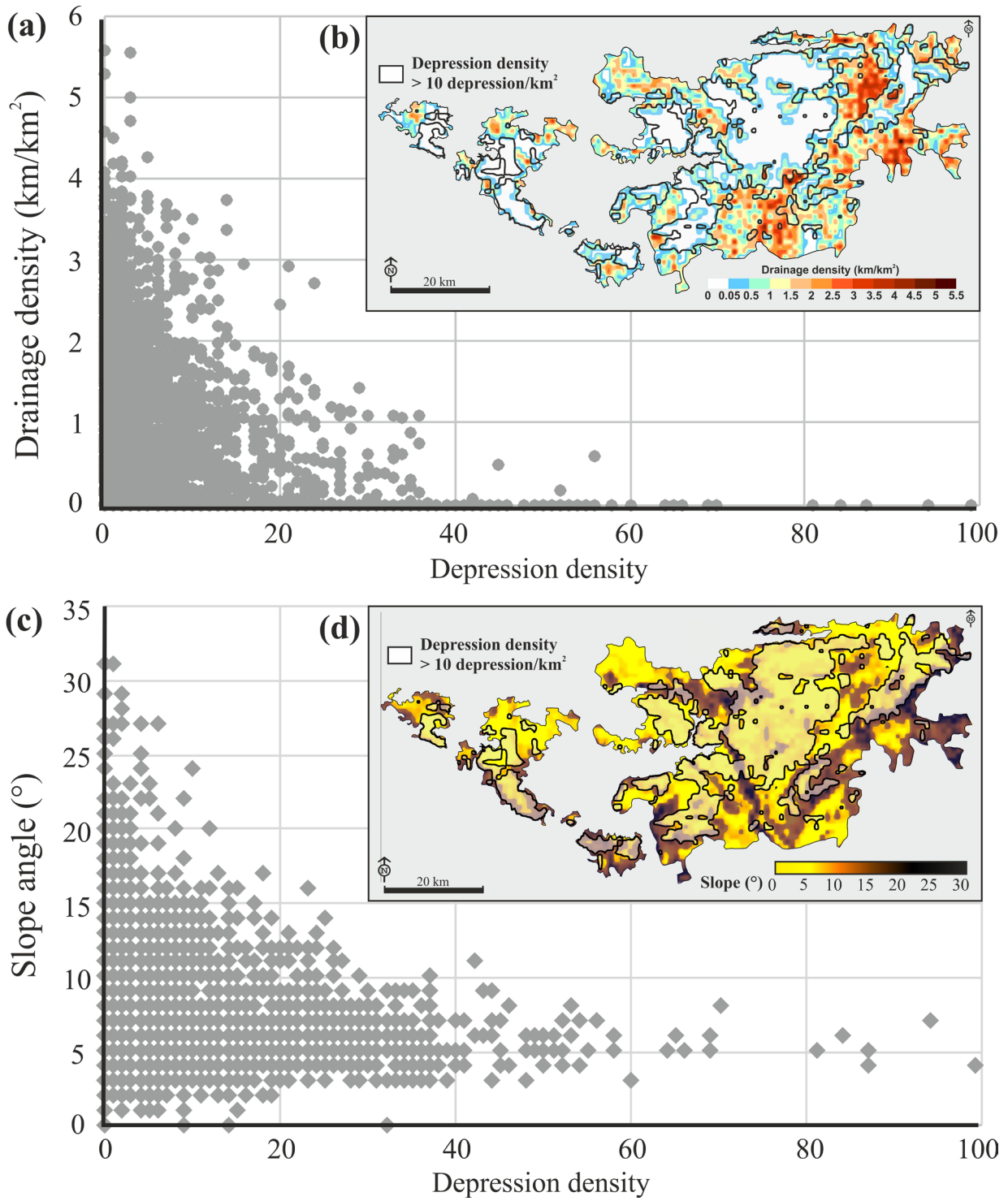


Figure 6. Reduction in depression density according to (a, b) drainage density and (c, d) slope angle.

7a does not reflect the spatial variations among the long-axis orientation within the area. As a result, more analysis is required and a set of gridded rose diagrams for each 25 km² is drawn with ReoRose software from the orientation of depressions. These diagrams are transferred to a map with Corel DRAW software to show the spatial variation of orientations. According to the gridded rose diagrams, while the orientation in the western sections rotates to

Table: Area, number of depressions, and density properties of neritic limestones in the study area.

Age	Area (% of study area)	Number of depressions	Density
Miocene	1757 km^2 (68.6%)	20,824 (69.1%)	11.8
Jurassic–Cretaceous	311 km^2 (12.1%)	5133 (17%)	16.5
Middle Triassic–Cretaceous	236 km^2 (9.1%)	2945 (9.5%)	12.4

ENE–WSW, in the northeast of the area it is NE–SW (Figure 7f). This distribution shows that the elongations of the karstic depressions form a curve. All rose diagram orientations are in harmony regardless of lithology and age. This situation shows that tectonic activity of the Ecemiş fault affected all lithological units in the same direction.

The tectonic characteristics of the area play a determinant role in the orientation of karstic depressions. Therefore, in order to explain the mean orientation of depressions within the study area and the curve in orientations observed, it is necessary to summarize the tectonic evolution of the area.

The Central Taurus Mountains were created by north–south compression of a carbonate platform in the Neo-Tethys Ocean between the African–Arabian and Eurasia plates beginning in the Middle Cretaceous (Biju-Duval et al., 1977; Livermore and Smith, 1984; Yazgan and Chessex, 1991; Bozkurt, 2001). After this period, the African plate was subducted to the north, while the Central Taurus mountains were exposed to compression, thickening, and uplift in five different periods during the Late Eocene–Early Oligocene, as (1), Middle Miocene (2), Late Miocene (3), Pliocene (4), and Early Pleistocene–present day (5) (Akay and Uysal, 1988; Schildgen et al., 2014; Karaoğlan, 2016). Additionally, stream profiles show that the Central Taurus underwent a multistage uplift instead of a continuous uplift (Altın, 2012; Schildgen et al., 2012).

In the Early Oligocene, the African–Arabian plate was subducted under the Anatolian plate, causing north–south compression, and the Central Taurus rose above sea level for the first time (Şengör and Yılmaz, 1981; Akay and Uysal, 1988; Jaffey and Robertson, 2001; Karaoğlan, 2016) (Figure 8a). In the Middle Miocene period, the N25°E striking, left-lateral strike-slip Ecemiş Fault Zone was created separating the Central and Eastern Taurus (Koçyiğit and Beyhan, 1998). After the Late Miocene, the Taurus Mountains began to uplift to their current form. Due to uplift in this period along the anticlinal (Şaroğlu et al., 1983; Akay and Uysal, 1988), a central N–S-oriented expansion occurred (Şengör, 1979; Şengör and Yılmaz, 1981; Özgül, 1976; Görür, 1985; Dewey et al., 1986; Dhont et al., 1999; Jaffey and Robertson, 2005). In addition, Cosentino et al. (2012) describe the study area as an asymmetric drape fold. Linked to this expansion, E–W oriented extension fracture systems began to form parallel to the fold axes (Figure 8b). Due to tectonic activity causing uplift, there was increased movement on the Beyşehir and Ecemiş faults. Formation of extension fractures, which began developing linked to compression in the Middle Miocene, increased in the Late Miocene period (Yetiş, 1984; Akay and Uysal, 1988) (Figure 8c).

In the Late Miocene–Pliocene, widespread fracture systems developed around the anticlinal fold axis in the center of the study area (Şaroğlu et al., 1983). These fractures ensured that depression density reached a maximum in the center of the study area, in other words, around the anticlinal surface. In this period, the area was completely above water (Schildgen et al., 2014). In the Pliocene, weak tectonic activity occurred, while in the last uplift stage 1.6 million years ago the break-off of the subducted plate beneath the Anatolian plate caused more rapid uplift to occur (Schildgen et al., 2014). In this period due to offset linked to left-lateral activity on the Ecemiş Fault, NE–SW orientation developed in the study area (Koçyiğit and Beyhan, 1999; Jaffey and Robertson, 2001). Together with folding of the continent, fractures formed and evolving depressions linked to these fractures were exposed to curving in the same orientation (Figure 8d). As the distance from the Ecemiş Fault increases, the effect of the fault lessens; in other words, it tends toward the initially formed fracture systems.

6. Conclusion

In this study, the spatial distribution patterns of karst depressions that emerged on a plateau in the west of the Bolkar Mountains were investigated and the effective tectonic and geomorphologic processes forming these patterns were described. The 30,132 karstic depressions identified were at an elevation of between 1315 and 2525 m in the study area. Maximum depression density reached 99 depressions/km^2 in the central section of the area, which is equivalent to the anticlinal surface. There are negative correlations between depression density, drainage density, and slope values. The karstic depressions in the study area were shaped by the subduction of the African–Arabian plate under the Anatolian plate, with the eastern section

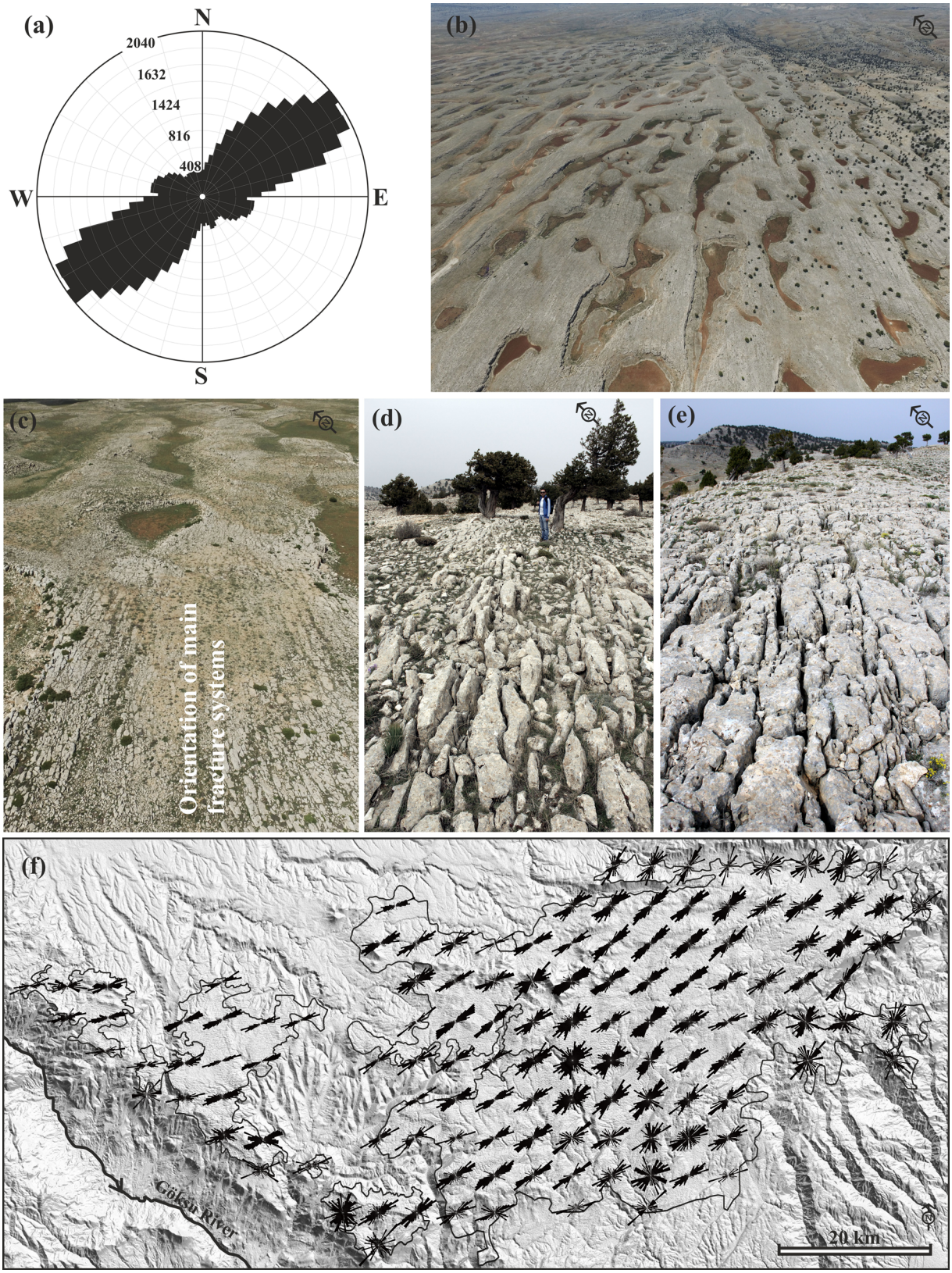


Figure 7. (a) Long axis orientation of all depressions in study area, (b) NE–SW-oriented depressions, (c, d, e) appearance of fracture systems affecting orientation of depressions, (d) orientation of depressions within 5 × 5 km grids.

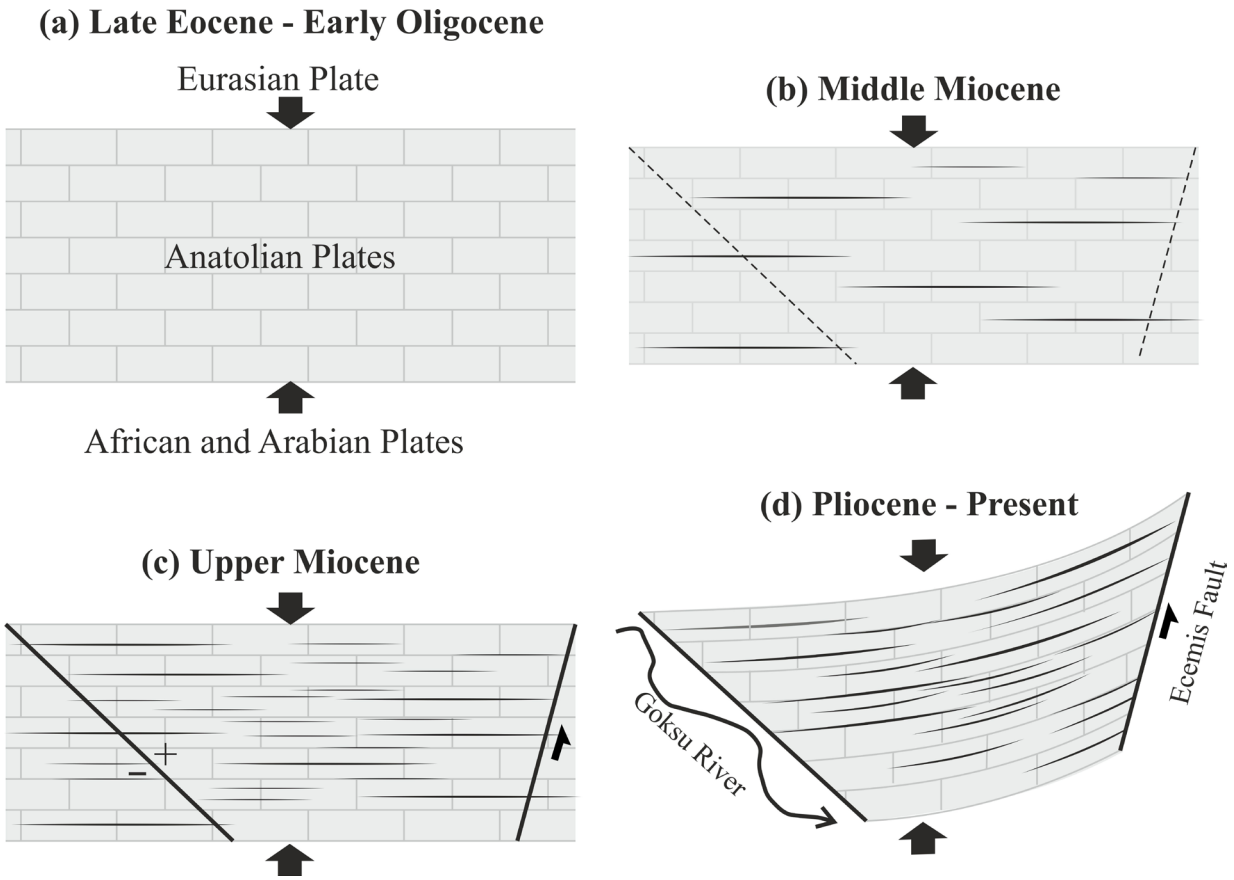


Figure 8. Formation and orientation change of fracture systems allowing development of karstic depressions within the tectonic evolution framework of the area.

gaining its current form due to fault offset along the left-lateral strike-slip Ecemiş Fault. The effect of the fault increases near the fault and is reduced away from it. In the east of the area, depression orientations are NE–SW, while in the western section there is a curve toward ENE–SWS.

Acknowledgment
This study was supported by the Scientific and Technological Research Council of Turkey (TÜBİTAK) (Project number: 115Y580). We express our sincere thanks for their financial support.

References

Akay E, Uysal S (1988). Post-Eocene tectonics of the central Taurus. MTA Bulteni 108: 57-68 (in Turkish with English abstract).

Altın TB (2012). Geomorphic signatures of active tectonic in drainage basins in the Southern Bolkar Mountains, Turkey. J Indian Soc Remote Sens 40: 271-285.

Ardos M (1992). Karaman çevresi ve güney kesimlerinde karstlaşma ve karstik şekiller. İÜ Edeb Fak Coğ Dergisi 3: 1-9 (in Turkish with English abstract).

Atabey E, Atabey N, Hakyemez A, İslamoğlu Y, Sözeri Ş, Özçelik NN, Saraç G, Ünay E, Babayiğit S. (2000). Mut-Karaman arası Miyosen Havzasının litostratigrafisi ve sedimantolojisi (Orta Toroslar). Maden Tetkik ve Arama Dergisi, 122: 53-72 (in Turkish with English abstract).

Benac C, Juracic M, Maticec D, Ruzic I, Pikelj K (2013). Fluviokarst and classical karst: examples from the Dinarics (Krk Island, Northern Adriatic, Croatia). Geomorphology 184: 64-73.

Biju-Duval B, Dercourt J, Le Pichon X (1977). From the Tethys Ocean to the Mediterranean Seas: a plate tectonic model of the evolution of the Western Alpine system. In: Biju-Duval B, Montadert, editors. Symposium on the geological history of the Mediterranean basins: Paris (Technip), pp. 143-164.

Bocic N, Pahernik M, Mihevc A (2015). Geomorphological significance of the paleodrainage network on a karst plateau: the Una–Korana Plateau, Dinaric karst, Croatia. Geomorphology 247: 55-65.

Bozkurt E (2001). Neotectonics of Turkey - a synthesis. Geodin Acta 14: 3-30.

Car J (2001). Structural bases for shaping of dolines. Acta Carsologica 30: 239-256.

Closson D, Karaki NA (2009). Salt karst and tectonics: sinkholes development along tension cracks between parallel strike-slip faults, Dead Sea, Jordan. Earth Surf Proc Land 34: 1408-1421.

Cosentino D, Schildgen, TF, Cipollari P, Faranda C, Gliozzi E, Hudáčková N, Lucifora S., Strecker MR. (2012). Late Miocene surface uplift of the southern margin of the Central Anatolian plateau, Central Taurides, Turkey. Geol Soc Am Bull 124: 133-145.

Daura J, Sanz M, Fornos JJ, Asensio A, Julia R (2014). Karst evolution of the Garraf Massif (Barcelona, Spain): doline formation, chronology and archaeo-palaeontological archives. J Cave Karst Stud 76: 69-87.

Day M (1983). Doline morphology and development in Barbados. Ann Assoc Am Geogr 73: 206-219.

Denizman C (2003). Morphometric and spatial distribution parameters of karstic depressions, Lower Suwannee River Basin, Florida. J Cave Karst Stud 65: 29-35.

Dewey JF, Hempton MR, Kid WSF, Şaroğlu F, Şengör AMC (1986). Shortening of continental lithosphere: the neotectonics of Eastern Anatolia young collision zone. In: Coward MP, Ries, AC editors. Collision Tectonics, Geol Soc Lond Spec Pub 19: 3-36.

Dhont D, Chorowicz J, Yürür T (1999). The Bolkar Mountains (Central Taurides, Turkey): a Neogene extensional thermal uplift. Geological Bulletin of Turkey 42: 69-87.

Doctor DH, Doctor KZ (2012). Spatial analysis of geologic and hydrologic features relating to sinkhole occurrence in Jefferson County, West Virginia. Carbonate Evaporite 27: 143-152.

Ekmekçi M, Nazik L (2004). Evolution of Gölpazarı-Huyuk karst system (Bilecik-Turkey): indications of morpho-tectonic controls. Int J Speleol 33: 49-64.

Elhatip H (1997). The influence of karstic features on environmental studies in Turkey. Environl Geol 31: 27-33.

Faivre S, Pahernik ZM (2007). Structural influences on the spatial distribution of dolines, Island of Brac, Croatia. Z Geomorphol 51: 487-503.

Faivre S, Reiffsteck P (1999). Spatial distribution of dolines as an indicator of recent deformations on the Velebit mountain range (Croatia). Géomorphologie: Relief, Processus, Environnement 2: 129-142.

Ford DC, Williams PW (2007). Karst Geomorphology and Hydrology, London, UK: Chapman and Hall.

Gams I (2000). Doline morphogenetic processes from global and local viewpoints. Acta Carsologica 29: 123-138.

Gedik A, Birgili Ş, Yılmaz H, Yoldaş R (1979). Mut-Ermenek-Silifke yöresinin jeolojisi ve petrol olanakları: Türkiye Jeoloji Kurumu Bülteni 27: 7-26 (in Turkish with English abstract).

Görür N (1985) Depositional history of Miocene sediments on the NW flank of the Adana basin. Proc. 6th Colloquium on Geology of the Aegean region, İzmir pp. 185-208.

Gunn J, Günay G (2004). Turkey. In: Gunn J editor. Encyclopedia of Caves and Karst Science. New York, NY, USA: Fitzroy Dearborn, pp. 1583-1589.

Günay G (2010). Case study: geological and hydrogeological properties of Turkish karst and major karstic springs. In: Kresic N, Stevanovic Z, editors. Groundwater Hydrology of Springs. Amsterdam, Netherlands: Butterworth-Heinemann, pp. 479-197.

Jaffey N, Robertson A (2001). New sedimentological and structural data from the Ecemis Fault Zone, southern Turkey: implications for its timing and offset and the Cenozoic tectonic escape of Anatolia. J Geol Soc London 158: 367-378.

Jaffey N, Robertson A (2005). Non-marine sedimentation associated with Oligocene– Recent exhumation and uplift of the Central Taurus Mountains, S Turkey. Sediment Geol 173: 53-89.

Jemcov I, Cupkovic T, Pavlovic R, Stevanovic Z (2001). An example of the influence of fault patterns on karst development. In: Günay G, Johnson KS, Ford D, Johnson AI, editors. Present State and Future Trends of Karst Studies: Proceedings of the 6th International Symposium and Field Seminar, Marmaris, Turkey, 17-26 September 2000, pp. 703-709.

Karaoğlan F (2016). Tracking the uplift of the Bolkar Mountains (south-central Turkey): evidence from apatite fission track thermochronology. Turk J Earth Sci 25: 64-80.

Klimchouk A, Bayarı S, Nazik L, Törk K (2006). Glacial destruction of cave systems in high mountains, with a special reference to the Aladaglar massif, Central Taurus, Turkey. Acta Carsologica 35: 111-121.

Koçyiğit A (1984). Güneybatı Türkiye ve yakın dolayında levha içi yeni tektonik gelişim. Türkiye Jeoloji Kurumu 27: 1-15 (in Turkish with English abstract).

Koçyiğit A, Beyhan A (1998). A new intracontinental transcurrent structure: the Central Anatolian Fault Zone, Turkey. Tectonophysics 284: 317-336.

Koçyiğit A, Beyhan A (1999). Reply to Rob Westaway's comment on 'A new intracontinental transcurrent structure: The Central Anatolian Fault Zone, Turkey. Tectonophysics 314: 481-496.

Lewin J, Woodward J (2009). Karst Geomorphology and Environmental Change. In: Woodward JC editor. The Physical Geography of the Mediterranean. Oxford, UK: Oxford University Press, pp. 287-317.

Livermore RA, Smith AG (1984). Some boundary conditions for the evolution of the Mediterranean region. In: Stanley DJ, Wezel CF editors. Geological Evolution of the Mediterranean Basin. Berlin, UK: Springer, pp. 83-110.

Mihljevic D (1994). Analysis of spatial characteristics in distribution of sink-holes, as a geomorphological indicator of recent deformation of geological structure. Acta Geogr Croatica 29: 29-36.

Nazik L (1986). Beyşehir Gölü yakın güneyi karst jeomorfolojisi ve karstik parametrelerin incelenmesi. Jeomorfoloji Dergisi 14: 65-77 (in Turkish with English abstract).

Özdoğan M (1999). Sedimentological evolution and depositional properties of the miocene deposits in the (NW) Mut basin. PhD, Hacettepe University, Ankara, Turkey.

Özgül N (1976). Some geological aspects of the Taurus orogenic belt (Turkey). Geological Bulletin of Turkey 19: 65-78.

Özgül N (1984). Stratigraphy and tectonic evolution of the central Taurides. In: Tekeli O, Göncüoğlu MC, editors. Geology of the Taurus Belt. Ankara, Turkey: MTA, pp. 77-90.

Özkale O, Yetiş C, İbilioğlu DE (2007). Stratigraphy of the Kozlar (Mut-Mersin) area. Çukurova University Journal of the Faculty of Engineering and Architecture 22: 261-273.

Öztürk MZ, Şimsek M, Utlu M (2015). Tahtalı Dağları (Orta Toroslar) karst platosu üzerinde dolin ve uvala gelişiminin CBS tabanlı analizi. Türk Coğrafya Dergisi 65: 59-68 (in Turkish with English abstract).

Plan L, Decker KD (2006). Quantative karst morphology of the Hochschwab plateau, Eastern Alps, Austria. Z Geomorphol 147: 29-54.

Sauro U (2013). Landforms of mountainous karst in the middle latitudes: reflections, trends and research problems. Acta Carsologica 42: 5-16.

Schildgen TF, Cosentino D, Bookhagen B, Niedermann S, Yıldırım C, Echtler HP, Wittmann H, Strecker MR (2012). Multi-phase uplift of the southern margin of the Central Anatolian plateau: a record of tectonic and upper mantle processes. Earth Planet Sc Lett 317-318: 85–95.

Schildgen TF, Yıldırım C, Cosentino D, Strecker MR (2014). Linking slab break-off, Hellenic trench retreat, and uplift of the Central and Eastern Anatolian plateaus. Earth-Sci Rev 128: 147-168.

Şaroğlu F, Boray A, Özer S, Kuşçu İ (1983). Orta Toroslar-Orta Anadolu'nun güneyinin Neotektoniği ile ilgili görüşler. Jeomorfoloji Dergisi, 11: 35-44 (in Turkish with English abstract).

Şenel M (2002). 1/500000 scaled geology map of Turkey, Adana sheet. Ankara, Turkey: General Directorate of Mineral Research and Exploration.

Şengör AMC (1979). The North Anatolian transform fault: its age, offset and tectonic significance. J Geol Soc London 136: 269-282.

Şengör AMC, Yılmaz Y (1981). Tethyan evolution of Turkey: a plate tectonic approach. Tectonophysics 75: 181-241.

Telbisz T, Dragušica D, Nagy B (2009). Doline morphometric analysis and karst morphology of Biokovo Mt (Croatia) based on field observations and digital terrain analysis. Hrvatski Geografski Glasnik 71: 5-22.

Theilen-Willige B, Malek HA, Charif A, El Bchari F, Chaïbi M (2014). Remote sensing and GIS contribution to the investigation of karst landscapes in NW-Morocco. Geosciences 4: 50-72.

Yazgan E, Chessex R (1991). Geology and tectonic evolution of the southeastern Taurides in the region of Malatya. Turk Assoc Petrol Geol 3: 1-42.

Yetiş C (1984). New observations on the age of the Ecemiş Fault. In: Tekeli O, Göncüoğlu MC, editors. Geology of the Taurus Belt. Int J Sym Proceedings, Ankara, pp. 159-164.